Matter and Radiation at Extremes

REVIEW ARTICLE | JUNE 26 2025

Short-range order in binary and multiple principal element alloys: A review

Special Collection: High Pressure Science 2025

Yuxin Liu ; Hongbo Lou ; Fei Zhang ; Zhidan Zeng ; Qiaoshi Zeng

Matter Radiat. Extremes 10, 043801 (2025)
https://doi.org/10.1063/5.0275123

Matter and Radiation at Extremes REVIEW pubs.aip.org/aip/mre

Editor's Pick

Short-range order in binary and multiple principal element alloys: A review

Cite as: Matter Radiat. Extremes 10, 043801 (2025); doi: 10.1063/5.0275123
Submitted: 10 April 2025 • Accepted: 28 May 2025 •
Published Online: 26 June 2025

Yuxin Liu,[1] Hongbo Lou,[1,2] Fei Zhang,[3] Zhidan Zeng,[1] and Qiaoshi Zeng[1,2,a)]

AFFILIATIONS

[1] Center for High Pressure Science and Technology Advanced Research, Shanghai 201203, People's Republic of China
[2] Shanghai Key Laboratory of Material Frontiers Research in Extreme Environments (MFree), Shanghai Advanced Research in Physical Sciences (SHARPS), Shanghai 201203, People's Republic of China
[3] Institute of High Energy Physics, Chinese Academy of Sciences, Beijing 100049, People's Republic of China

Note: Paper published as part of the Special Topic on High Pressure Science 2025.
[a)] **Author to whom correspondence should be addressed:** zengqs@hpstar.ac.cn

ABSTRACT

Multiple principal element alloys (MPEAs), also known as high-entropy alloys, have attracted significant attention because of their exceptional mechanical and thermal properties. A critical factor influencing these properties is suggested to be the presence of chemical short-range order (SRO), characterized by specific atomic arrangements occurring more frequently than in a random distribution. Despite extensive efforts to elucidate SRO, particularly in face-centered cubic (fcc) 3*d* transition metal-based MPEAs, several key aspects remain under debate: the conditions under which SRO forms, the reliability of characterization methods for detecting SRO, and its quantitative impact on mechanical performance. This review summarizes the challenges and unresolved issues in this emerging field, drawing comparisons with well-established research on SRO in binary alloys over the past few decades. Through this cross-system comparison, we aim to provide new insights into SRO from a comprehensive perspective.

I. INTRODUCTION

High-entropy alloys (HEAs) and medium-entropy alloys (MEAs), collectively termed multiple principal element alloys (MPEAs), represent a novel alloy system composed of three or more principal elements (each with atomic fractions within the range of ~5%–35%) and named after their high configurational entropy. In conventional metallurgical paradigms, alloys typically employ one or two principal elements as the solvent, supplemented by small quantities of other elements as solutes (constituting merely a few atomic percent) to tailor specific material properties. Conventionally, alloy systems containing multiple concentrated elements, like the well-known Cantor alloy (CrMnFeCoNi) and Senkov alloy (TiZrHfNbTa), usually have difficulty forming stable single-phase solid solutions. Instead, they tend to form brittle intermetallic compounds. Surprisingly, the systems represented by these two types of alloys, namely 3*d* transition metal MPEAs and refractory MPEAs, have been found to form rather stable single-phase structures with simple crystal lattices, exhibiting exceptional mechanical properties.[1–5] The stability of these phases is largely attributed to the competition between entropy and enthalpy in MPEAs.[6,7] High configurational entropy arising from compositional complexity promotes structural disorder, whereas differences in bonding enthalpies (or atomic pair preferences) between constituent elements typically favor ordered intermetallic phases. The interplay and delicate balance between entropy and enthalpy effects result in relatively stable, near-disordered solid solutions.

Although the high-entropy effect induces substantial compositional disorder in MPEAs with atoms randomly occupying lattice sites in simple face-centered cubic (fcc) or body-centered cubic (bcc) lattices, atomic size differences and enthalpy variations among elements inevitably result in short-range order (SRO).[8] Unlike long-range order (LRO), where atoms occupy specific lattice positions in a periodic manner, SRO is confined to the first or second nearest-neighbor atomic shells, reflecting localized deviations from random

atomic distributions. Strictly speaking, SRO is a thermally induced infinitesimal concentration fluctuation and is directly related to chemical pair correlations, whereas the preferential local ordering of elements more than a few nearest-neighbor atom spacings can be termed local chemical order (LCO).[9] In numerous studies, the concepts of LCO and SRO are often used interchangeably, with no strict distinction made between them. However, it is important to emphasize that SRO is fundamentally different from both nanosized phase segregation and nanoscale compositional undulation, even though these structures frequently coexist in numerous systems.[4,10,11] Nanosegregated phases can reach several nanometers and possess clearly defined lattice structures. By contrast, SRO/LCO should be recognized as sub-nanometer-scale ordered configurations (within a size of 2 nm) and, in the strictest sense, are confined to the nearest-neighbor atomic shells. Nanoscale compositional undulations simply reflect spatial compositional variations within the material system, which do not necessarily signify any specific type of atomic ordering.[12]

Recently, atomic SRO in MPEAs, sometimes alternatively termed chemical short-range order (CSRO) to distinguish it from potential magnetic SRO, has garnered significant research interest. This attention stems not only from its intrinsic connection to structural characteristics of compositional disorder and complex entropy–enthalpy competition in MPEAs, but also from its potential to create highly tunable properties for engineering applications.[2,3,13] In particular, in fcc-structured 3*d* transition metal MPEAs exemplified by CrCoNi, modulation of the degree of SRO has been demonstrated to substantially enhance mechanical performance through altered dislocation slide pathways and modified local energy landscapes, even achieving remarkable synergistic improvements in both strength and ductility.[1,14,15] However, fundamental debates persist regarding SRO in MPEAs, with even its existence and effects on properties being doubted.[16–20] Neither experimental nor calculational approaches have yet been able to provide a convincing conclusion.[21]

Revisiting simpler binary alloy systems reveals a well-established understanding of SRO from extensive previous research. Comprehensive experimental methods have been developed to quantify SRO in binary alloys. A detailed discussion of these methods, as well as attempts to characterize SRO in MPEAs, will be presented in subsequent sections of this review. We will highlight similarities and differences in SRO between typical binary alloys and MPEAs and review the latest advances in the characterization of SRO in MPEAs, aiming for a systematic overview of this emerging research field.

II. SRO PARAMETERS

First, to understand SRO quantitatively, a short introduction to the relevant SRO parameters that define the degree of SRO should be essential. Decades ago, seminal investigations of Cu–Au and Cu–Zn systems by Cowley, Keating, and Warren[22–24] established the Warren–Cowley (WC-SRO) parameters, which constitute a critical metric for quantifying SRO intensity that has been used since the 1950s:

$$\alpha_{lmn}^{AB} = 1 - \frac{P_{lmn}^{AB}}{c_B} = 1 - \frac{P_{lmn}^{BA}}{c_A},$$

where c_A and c_B are the concentrations of elements A and B, respectively, and P_{lmn}^{AB} is defined as the probability of finding a B atom at a position $\boldsymbol{R}_{lmn} = l\boldsymbol{a}_1 + m\boldsymbol{a}_2 + n\boldsymbol{a}_3$ from a center atom A (where $\boldsymbol{a}_1$, $\boldsymbol{a}_2$, $\boldsymbol{a}_3$ are lattice vectors, and l, m, n are fractional coordinates). When $\alpha_{lmn}^{AB} = 0$, the binary system is completely random. When α_{lmn}^{AB} lies in the range $0 < \alpha \leq 1$, it indicates a preference for homoatomic coordination (A–A or B–B pairs) over random distribution at the lattice site R_{lmn}, whereas $\alpha_{lmn}^{AB} < 0$ signifies a preference for heteroatomic coordination (A–B pairs) at the same site.

The WC-SRO parameters can be directly quantified by single-crystal diffuse scattering experiments, through integrated intensity of these diffuse scattering features:

$$I_{\mathrm{SRO}} \propto \alpha(x,k) = \sum_{lmn}^{n_R} \alpha_{lmn}(x) e^{i\boldsymbol{k}\cdot\boldsymbol{R}_{lmn}},$$

where I_{SRO}, the intensity of the diffuse scattering due to SRO, is proportional to the Fourier transform of the WC-SRO parameters, and $\boldsymbol{k}$ is the composition wavevector.[24,25]

The WC-SRO parameters are only applicable to binary systems, and in multiple-component systems, there will be multiple types of atomic pairs. A simple formula describing SRO for these systems can be derived from the WC-SRO parameters, and we can thus obtain the pairwise short-range order (PM-SRO) parameters

$$\alpha_m^{AB} = \frac{P_m^{AB} - c_B}{\delta_{AB} - c_B},$$

where m is the mth atom-shell around center atom A, and P_m^{AB} is the probability of finding a B atom around an A atom in shell m.[26] For multiple-principal-element systems, the PM-SRO parameters are the most widely used SRO parameters for extracting information from scattering experiments, although PM-SRO accounts for pair correlations only without ternary or higher-order multicomponent correlations (i.e., correlations between sets of elements).

Building upon the PM-SRO framework, more complex and precise formulations such as the generalized multicomponent short-range order (GM-SRO) parameters can be developed. The GM-SRO parameters are defined in terms of structural pair correlations by retaining the concept of neighbor shells and are able to include higher-order compositional correlations.[27] The GM-SRO parameters are given by

$$\alpha^m_{\{B_j\}_{j=1}^k\{C_l\}_{l=1}^h} = (-1)^{\left(1+\delta_{\{B_j\}_{j=1}^k\{C_l\}_{l=1}^h}\right)} \frac{p^m_{\{B_j\}_{j=1}^k\{C_l\}_{l=1}^h} - X_{\{C_l\}_{l=1}^h}}{\delta_{\{B_j\}_{j=1}^k\{C_l\}_{l=1}^h} - X_{\{C_l\}_{l=1}^h}},$$

where $p^m_{\{B_j\}_{j=1}^k\{C_l\}_{l=1}^h}$ represents the probability that in the mth shell around any atom of the set $\{B_j\}$ there occurs an atom belonging to another set $\{C_l\}$, and this probability can be extracted as

$$p^m_{\{B_j\}_{j=1}^k\{C_l\}_{l=1}^h} = \frac{\sum_{j=1}^k \left(N_{B_j} \sum_{l=1}^h p^m_{B_jC_l}\right)}{\sum_{j=1}^k N_{B_j}},$$

where N_{B_j} is the number of atoms of type B_j.

If higher-order compositional correlations are neglected, PM-SRO and GM-SRO remain equivalent. However, to accurately

describe potential higher-order correlations, the definition of GM-SRO requires a significantly larger number of parameters. Specifically, the number of GM-SRO parameters is equal to the total number of all possible combinations of possible elements in the sets $\{B_j\}$ and $\{C_l\}$. To model a binary system, the definition of PM-SRO requires four parameters, while GM-SRO requires nine parameters. In a ternary system, the number of PM-SRO parameters becomes 9, and the number of GM-SRO parameters becomes 49. For a typical high-entropy system with five components, 961 parameters are needed to define GM-SRO. Such complexity significantly constrains the application of diffuse scattering experiments for the quantitative investigation of GM-SRO in multicomponent systems. Current experimental approaches for determining GM-SRO parameters in multicomponent systems rely predominantly on the synergistic integration of three-dimensional atom probe tomography (3D-APT) and computational simulations.[27–29]

Following this establishment of SRO parameters and the basic methods for their experimental determination, a comparative analysis of SRO in binary alloys and MPEAs can now be systematically undertaken.

III. SRO IN BINARY ALLOYS

A. Classification of SRO in binary alloys

As mentioned above, SRO in binary alloys has been a fundamental crystallographic research topic since its initial investigation in the mid-twentieth century, and decades of research have established a comprehensive framework that enables the identification and classification of SRO from both thermodynamic and structural perspectives. In binary systems, SRO generally exhibits strong correlations with either LRO or phase separation (LRO can also be termed coherent phase separation, and the "phase separation" here then refers to incoherent phase separation).[30–32] For numerous binary alloys exhibiting LRO or phase separation that are stable at low temperatures, SRO is typically interpreted as either a residual or a precursor state of LRO at higher temperatures.[33] Above the critical temperature of order–disorder transition in these systems, while periodic LRO disappears in bulk samples, measurable SRO still persists. The tendency to the formation of SRO in A–B binary systems manifests as either "ordering" (preferential A–B bonding) or "clustering" (A–A/B–B bonding), although strict definitions may exclude clustering from SRO categorization. Nevertheless, both structures will be discussed here.

The relationship between SRO and LRO depends fundamentally on the energy competition governed by specific composition and temperature conditions, and this energetic relationship can provide a classification framework for SRO.[25] On the basis of thermodynamic comparisons between the mixing enthalpy ΔH_{mix} of disordered random systems, the formation enthalpy ΔH_{ord} of ordered structures, and the strain energy ΔH_{CPS} necessary to maintain coherence between separated phases, and considering the incoherent phase separated state as the zero-energy reference, SRO in binary alloys can be classified into several distinct regimes. The two most common types are as follows:

1. For $\Delta H_{\mathrm{ord}} < \Delta H_{\mathrm{mix}} < 0 < \Delta H_{CPS}$, there are alloys of type I, such as the Cu–Au system, in which ordering-type SRO is favored and the stable random alloy is able to lower its energy such that SRO evolves into LRO.
2. For $0 < \Delta H_{CPS} < \Delta H_{\mathrm{ord}} < \Delta H_{mix}$, there are alloys such as the Cu–Ag system, identified as type V in Ref. 25, in which clustering-type SRO is favored and the unstable random alloy is able to lower its energy such that the SRO evolves into phase separation.

These two types of alloys can occur in most compound-forming systems and most phase-separating systems, and the SRO of these alloys can evolve straightforwardly into LRO with the same atomic arrangement.

In addition, three further types of SRO exist, which are relatively less prevalent:

3. For $\Delta H_{\mathrm{ord}} < 0 < \Delta H_{mix} \approx \Delta H_{CPS}$, there are alloys of type II, such as the Al–Mg system, in which ordering-type SRO is favored, and the unstable random alloy is able to lower its energy such that SRO evolves into LRO.
4. For $0 < \Delta H_{\mathrm{ord}} < \Delta H_{CPS} < \Delta H_{mix}$, in alloys such as semiconductor alloy systems and the Ti–V system, ordering-type SRO is favored, and the unstable random alloy is able to lower its energy such that the SRO evolves into phase separation.
5. For $0 < \Delta H_{\mathrm{ord}} \approx \Delta H_{CPS} < \Delta H_{mix}$, there are alloys such as the Ni–Cu system in which both ordering-type and clustering-type SRO are favored, and the unstable random alloy is able to lower energy via two pathways to LRO or phase separation.[34–37]

The existence of these three uncommon types of binary system with SRO helps us to understand how ordering-type SRO can coexist with phase-separating LRO and unstable random alloy states.

From the above discussion, it can be deduced that the composition wavevectors characterizing SRO and LRO may not necessarily coincide. Specifically, the reciprocal-space positions of SRO features observed in diffuse scattering experiments do not always correspond to those of the ultimately stabilized long-range ordered phase.

An alternative classification framework based on structural characteristics can be used to divide SRO into three types: statistical order, a microdomain model, and a disperse model,[38,39] as shown schematically in Fig. 1. Statistical order is similar to the ordering found in some glasses, where the occupation in any neighboring shell around the central atom of a specific type fluctuates around a certain value, and with increasing distance from the center atom, atomic arrangements become statistically uncorrelated without forming distinct ordered domains. The statistical order corresponds to a homogenous order throughout the bulk sample. By contrast, order in the microdomain and disperse models exhibits identifiable domain interfaces despite limited spatial extent (typically several atomic shells). The distinction lies in stoichiometric variation: order in the microdomain model maintains matrix stoichiometry with local arrangement preferences (e.g., Cu–Au-type ordering), whereas order in the disperse model exhibits stoichiometric deviations between ordered regions and matrix (e.g., Fe–Al-type ordering), with extreme cases manifesting as clustering of atoms. A potential fourth model of SRO, the lattice defect model, refers to metastable states where compositional variations arise because of lattice defects and a more considerable degree of order is found close to these lattice defects.[38]

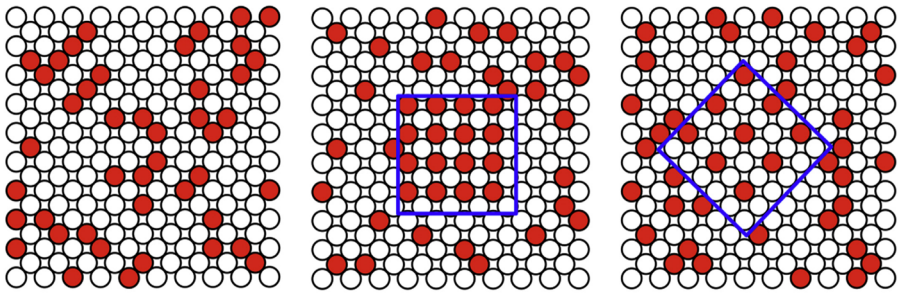

FIG. 1. Schematic representations of the three types of SRO that can exist stably in a crystalline alloy system: (a) statistical order; (b) microdomain model; (c) disperse models. In each case, the average unit cell of each box is the same. In the disperse and microdomain models, the ordered region is outlined in blue.[40]

B. Some typical binary alloys

There are hundreds of binary alloy systems with different solute concentrations. Here, we will only focus on some prototype binary alloys and relevant characterization methods for better understanding and comparison.

The Cu–Au system, especially Cu_3Au alloy, represents one of the most widely studied SRO-containing binary systems. The SRO of Cu_3Au can be classified as type I (ordering-dominant type) from an energy perspective, and it corresponds structurally to the microdomain model.[25,39] In Cu_3Au alloy, the $L1_2$ ordered phase is stable at low temperatures (below ~670 K), with Au atoms occupying the corner site and Cu atoms occupying the face center site of the fcc unit cell.[22,23] At ~660 K, $L1_2$-structured Cu_3Au undergoes a diffusion-controlled rapid order–disorder transition and exhibits a disordered fcc phase above the critical temperature, while a certain degree of SRO is still retained. Among binary alloys, SRO in Cu_3Au has been studied for the longest time, and methods for characterizing SRO have also been most comprehensively developed for Cu_3Au.[41–43] Through multiple experimental approaches, including diffuse scattering experiments, resistivity measurements, and thermodynamic characterization, both the long-range order–disorder transition and subsequent evolutions of SRO have been thoroughly investigated, yielding largely consistent results. Generally, under equilibrium conditions above ~870 K, the SRO in Cu_3Au is essentially thoroughly disrupted, manifesting as a completely disordered random solid solution. Within the temperature range of ~670–870 K, although the disordered fcc matrix persists in Cu_3Au, the equilibrium SRO concentration gradually increases with decreasing temperature.[43] This gradual enhancement continues until the critical temperature of ~670 K is reached, at which a sudden intensification of the degree of SRO occurs, followed by rapid formation of LRO.

The Ni–Cr alloy system, particularly Ni_2Cr, has recently garnered some attention owing to its similarity in properties to the representative 3*d* transition MPEA, CrCoNi.[44] Among Ni–Cr alloys, both $L1_2$-type Ni_3Cr and Pt_2Mo-type Ni_2Cr have been considered, although only the latter has been investigated experimentally.[38,45] The Pt_2Mo structure has an orthorhombic unit cell with $a = a_0/\sqrt{2}$, $b = 3a_0/\sqrt{2}$, $c = a_0$, where a_0 is the lattice parameter referring to the fcc unit cell. In contrast to the rather rapid ordering or disordering kinetics in Cu–Au, which takes less than a few hours for annealing, the formation of LRO in Ni–Cr is quite slow, and the annealing time can be up to hundreds of hours at 673–823 K.

In addition, the Fe–Al system, in which Al atomic concentrations are typically below 20%, has been extensively studied as a representative system exhibiting SRO according to the dispersed model.[28,46–48] This system demonstrates a tendency for phase separation, forming a bcc-Fe matrix and $D0_3$-type Fe_3Al ordered structure when annealed in the temperature range 523–673 K. The ordered Fe_3Al phase possesses a face-centered arrangement, with its unit cell constructed through the stacking of eight simple bcc subcells. For both Ni–Cr and Fe–Al systems, the existence of SRO has been consistently verified not only through diffuse scattering experiments, but also via electrical resistivity measurements.

Finally, the Fe–Cr system exhibits composition-dependent short-range ordering or clustering behavior that is critically influenced by both thermal treatment and chromium concentration.[49–51] At low Cr concentrations (<5 at. %), Fe–Cr atomic pairs exhibit negative WC-SRO parameters, indicating a tendency for SRO formation. By contrast, within the higher Cr concentration range (5–15 at. %), annealing at 1023–1123 K induces the development of two types of short-range clustering: Fe-rich and Cr-rich nanoscale domains. The critical Cr concentration for this ordering-to-clustering transition has been experimentally determined to lie between 9 and 11 at. %.[50,52,53] Although conventional X-ray diffuse scattering faces significant challenges in resolving SRO or clustering tendencies because of the similar diffraction contrast between Fe and Cr, other advanced characterization methods, such as neutron scattering and Mössbauer spectroscopy, have proven effective in elucidating these features. Notably, these methodologies have also been successfully extended to Fe–Al alloys.[54]

C. Characterization of SRO by scattering techniques

Diffuse scattering experiments utilizing X rays, electrons, or neutrons have long served as the principal method for SRO investigation, owing to their capability to directly reveal structural information in reciprocal space.[38,43,55–58] In reciprocal space, SRO manifests as diffuse intensity away from Bragg scattering peaks, with reciprocal distribution characteristics dependent on the preferred structure and SRO types, and such diffuse intensities can be collected by measuring complete 2D planar sections of scattering data from aligned single crystals.[25,38] The positions of the diffuse maxima of SRO are

usually close to the superstructure positions, while sometimes the Fermi surface can modulate the diffuse scattering and induce a splitting of the diffuse maxima.[38,56,59,60] As typical diffuse scattering intensities are usually 10^3–10^4 lower than those of Bragg peaks, achieving optimal signal quality requires both a clean background and incident beams with large flux. Conventional laboratory-based powder X-ray diffraction techniques could be employed, but are not recommended for SRO characterization, and a rotational sample stage is necessary to get enough information.[61] High-quality single-crystal samples are also required for practical diffuse scattering experiments capable of resolving SRO features. Under the condition that all prerequisites are met, as we mentioned above, the WC-SRO parameters can be extracted from the integrated intensity of these diffuse scattering features.

In addition to the traditional characterization methods mentioned above, recent experimental studies combining synchrotron X-ray techniques with reverse Monte Carlo (RMC) fitting have demonstrated that quantitative analysis of SRO in Cu_3Au can be achieved through total scattering experiments across the high-q range, even on powder samples, followed by pair distribution function (PDF) analysis.[39,40] While extended X-ray absorption fine structure (EXAFS) spectroscopy has been proposed as a promising SRO characterization tool because of its element-specific capability to probe real-space radial distribution differences within the few nearest atomic shells, practical implementations have also shown sensitivity in detecting SRO variations.[46,62–65] If the SRO of a binary alloy corresponds to a Mössbauer isotope suited for resonant absorption, such as ^{57}Fe, the local arrangement around the specific atoms can also be determined. In the Fe–Cr and Fe–Al systems, Mössbauer spectroscopy has revealed short-range ordering or clustering through analysis of the relative spectral area corresponding to the probability of the specific atomic configurations.[50,53,54,66,67]

Most of diffuse scattering experiments have been performed employing X-ray or electron beams, while diffuse neutron scattering, with time-of-flight scattering data collected from multiple detectors, can sometimes reveal higher diffuse scattering intensities from locally ordered structures, since the neutron scattering coefficients are not related to the atomic number Z.[61] For the SRO in systems composed of neighboring transition elements such as Fe–Cr and Ni–Cr, neutron diffuse scattering has proven to be a more powerful tool for characterizing the existence of SRO in those alloys.[49,52,66]

D. Characterization of SRO by resistometry and calorimetry

In addition to characterization based on scattering experiments, resistivity measurements serve as another commonly employed approach for investigating SRO in binary alloys.

In fact, the effects of SRO on resistivity had been experimentally observed even before the formal conceptualization of SRO. Initially, the anomalous resistivity changes observed at low-temperature annealing without phase transitions in various binary alloys such as the Ni–Cr, Fe–Al, and Ni–Al systems were termed the "K-state" or "complex state."[68–71] Correlation between these phenomena and SRO or LRO was subsequently established.[72,73] Generally, structural disorder such as impurities and defects is well known to scatter conduction electrons and increase electrical resistivity compared with perfectly ordered crystals, as described by Matthiessen's rule. Conversely, the formation of LRO will reduce scattering cross sections, thereby lowering resistivity. While conventional annealing eliminates structural defects in an alloy, thereby reducing its electrical resistivity, the K-state describes the behavior in those alloys where electrical resistance exhibits an anomalous rise with increasing annealing temperature. Actually, K-state has been taken as an indicator for the presence of SRO in the disperse model with highly ordered particles in a partially ordered matrix, and the formation of dispersed SRO can enhance the scattering of conduction electrons, thereby increasing the electrical resistivity.[21,38] For other types of SRO, such as that of the microdomain model in Cu_3Au, analysis of resistivity variations has become a prevalent method for monitoring the evolution of SRO, since the electrical resistivity decreases during the formation of SRO.[74–76]

Thermal analysis has also been demonstrated to serve as an effective approach for characterizing the evolution of LRO and SRO in binary alloys, especially in Cu_3Au, with its rapid rate of ordering. During the ordering process, the configurational entropy of the sample decreases, while the residual ordering enthalpy gradually approaches zero. Differential scanning calorimetry (DSC), a technique detecting heat flow variations during temperature modulation, has been extensively employed for studying the thermodynamic mechanism of SRO in Cu_3Au. In Cu_3Au, although the endothermic peak observed around ~670 K in DSC clearly demonstrates its long-range order–disorder transition, the enthalpy changes associated with the evolution of SRO in the disordered state above ~670 K, as derived from DSC curve integration, remain remarkably subtle.[77] Nevertheless, comparison of exothermic signals corresponding to long-range ordering in disordered Cu_3Au samples quenched from different temperatures confirms the evolution of SRO at elevated temperatures. Recent advances have enabled successful isolation of the effect of SRO on configurational entropy in disordered Cu_3Au through sophisticated differentiation between vibrational and configurational entropy at high temperatures.[78] An alternative methodology involves relaxation calorimetry with the Physical Property Measurement System (PPMS, Quantum Design) for specific heat measurements in the low-temperature range (0–300 K).[78,79] When combined with high-temperature heat capacity data from DSC, this approach enables the separation of configurational entropy contributions specifically related to SRO from vibrational entropy components.[78–80] In addition, although the ordering rate in the Ni–Cr system is quite slow, a thermal signal corresponding to the formation and destruction of SRO in Ni–33 at. %Cr and Ni–20 at. %Cr can still be captured in DSC measurements, although the exothermal and endothermal peaks of DSC curves are rather broad and weak.[81–83]

IV. FORMATION OF SRO IN MPEAs

A. Classification of SRO in MPEAs

Although the aforementioned classification frameworks derived from binary alloy systems are informative, it must be emphasized that they cannot be directly extrapolated to complex MPEAs. In binary systems, ordering and clustering are well defined and mutually exclusive phenomena. In MPEAs, however, this distinction becomes considerably blurred. The inherent complexity of local chemical environments and synergistic interactions between multiple principal elements renders thermodynamic classification

schemes for binary alloys, typically based on pairwise atomic energy competitions, inapplicable to MPEAs.[9,21] With regard to structural classification of SRO models, in the case of binary alloys, straightforward identification of SRO types (e.g., statistical ordering, microdomain model, or disperse model) is possible through their direct correlation with corresponding long-range ordered structures that emerge from SRO evolution at lower temperatures. By contrast, while the characterization of SRO structural types in MPEAs presents greater challenges, systematic experimental and computational investigations remain both feasible and necessary.

B. SRO–LRO transition in MPEAs

Notably, unlike binary systems, where SRO often evolves into LRO or incoherent phase separation, most MPEAs exhibit no clear SRO–LRO transition pathways, owing to intense entropy–enthalpy competition.[84] The absence of LRO constitutes one of the fundamental distinctions between MPEAs and traditional concentrated binary alloys with SRO, while incoherent phase separation is not so rare, since some of the single-phase MPEAs are metastable and will decompose after long-time annealing.[85–89] Although a few exceptions exist where ordered phase precipitation can be induced through temperature or pressure manipulation in specific compositions, these systems inherently lack a stable disordered single-phase matrix containing pre-existing ordered nuclei that facilitate precipitation.[90–93] Conversely, some MPEAs with highly stable single-phase LRO structures (e.g., B2 phases), such as Al_xCrFeCoNi with high Al concentration and $(TiZrHf)_{50}Co_{25}Ni_{25}$, exhibit no obvious order–disorder transitions within their solid-state ranges.[5,66,94–96]

Nevertheless, the absence of SRO–LRO transition does not preclude tunability of the degree of SRO within MPEAs. For most MPEAs with stable fcc/bcc lattice structures, high-temperature annealing near the melting point is typically employed to maximize configurational entropy and minimize SRO.[14,97,98] It should be noted that SRO will not be destroyed entirely in these high-temperature annealed systems with substantial atomic size mismatches or bonding heterogeneity driven by localized strain energy fluctuations and electronic interactions.[99–102] In 3*d* transition metal MPEAs, which consist of magnetic elements, magnetic interactions are frequently proposed as an additional driving force to induce the formation of SRO.[103–106] Even in MPEAs composed of neighboring similar elements, weak but detectable SRO survives after high-temperature annealing.[15] Experimental observations of such residual SRO may partially reflect quenching rate limitations that permit weak but rapid short-range ordering.[107,108] Both simulations and experiments confirm the enhancement of SRO upon cooling and annealing at lower temperatures, consistent with suppression of the entropy effect.[14] However, neither approach has conclusively identified a critical annealing temperature corresponding to the maximum SRO formation, and this has become a fundamental knowledge gap in this topic.

C. Annealing-induced SRO in MPEAs

The experimental incompatibility between LRO and SRO, coupled with challenges in identifying the temperature of short-range ordering peak, manifests as inconsistent heat treatment protocols across studies. As an example, we will take the ternary medium-entropy alloy CrCoNi, which is an fcc-structured Cantor-derived MPEA extensively investigated for its highly tunable SRO and outstanding mechanical performance. It should be noted that all the associated experimental procedures have consistently employed the aforementioned high-temperature annealing near the melting point as a prerequisite homogenization treatment to ensure homogenization of samples and suppression of SRO, and it can be supposed that the states in these initial samples (or homogenized samples) are consistent. The heat treatment parameters implemented across these studies involved sustained annealing at temperatures ranging from 1373 to 1473 K for tens to hundreds of hours. Yin *et al.*[16] attempted to induce SRO by annealing homogenized samples at 873–973 K for up to 384 h. Their results indicated either minimal SRO formation or negligible SRO-induced yield strength enhancement, and the latter conclusion was corroborated by Inoue *et al.*[109] under similar conditions. Zhang *et al.*,[2,110] however, reported contradictory findings, demonstrating that a short-range ordering peak and remarkable yield strength can be achieved after annealing for more than 100 h at 1173–1273 K. Zhou *et al.*[111] also observed detectable SRO following annealing at 873 or 1273 K for just 1 h, while Li *et al.*[18,19] identified annealing at 673 K for more than 500 h as optimal for SRO maximization and mechanical enhancement. Han *et al.*[112] even reported that SRO could be a ubiquitous feature that is insensitive to cooling rates and annealing treatments. Such stark discrepancies arising from varied characterization approaches and thermal histories pose fundamental challenges to understanding SRO formation mechanisms in MPEAs.

For fcc-structured 3*d* transition metal MPEAs such as CrCoNi, a critical unresolved question remains: Could lower annealing temperatures enable unprecedented SRO enhancement or even unobserved LRO formation? This directly relates to a broader enigma: Does an optimal SRO formation temperature window exist, or does equilibrium SRO concentration progressively increase with cooling until potential LRO emergence? Computational studies tentatively support the latter scenario.[14,113] However, experimental validation remains obstructed by the well-known Arrhenius equation:

$$k = A \exp\left(-E/RT\right),$$

where k is the ordering rate, A is a pre-exponential factor, R is the gas constant, T is the absolute temperature, and E is the activation energy. A reduction in annealing temperature will exponentially decelerate atomic rearrangement, rendering kinetic barriers insurmountable for achieving high SRO levels within practical timescales. Testing this hypothesis would require multi-year annealing experiments, a feat previously accomplished in metallic glass and traditional alloy research, but currently unfeasible for the nascent MPEA field.[72,114–116] The huge timescale limitations fundamentally constrain experimental verification of equilibrium SRO behavior in MPEAs at lower temperatures.

However, a recent work by Bacurau *et al.*[44] has proposed 748 K as a potential critical temperature for optimized SRO formation in CrCoNi, analogous to long-range ordering temperatures in $CrNi_2$, while demonstrating that 973 K is sufficient to completely suppress SRO development and erase prior ordering thermal histories. These

findings suggest an alternative paradigm: SRO formation in MPEAs may be thermodynamically favored within a specific intermediate temperature window, with maximum ordering being achievable only under optimized thermal conditions. Deviation from this window, even with prolonged annealing to enable atomic diffusion, results in minimal SRO formation.

This contrasts sharply with conventional homogenization conditions in MPEA research. Traditional SRO-suppression protocols, as mentioned above, typically involve days-long annealing at 1373–1473 K followed by rapid quenching, whereas Bacurau *et al.*[44] unexpectedly achieved homogenization at dramatically lower temperatures. Their latest conclusions indicate that complete SRO formation/dissolution cycles can occur within a temperature region of 300 K, fundamentally challenging existing thermal processing assumptions.

In the case of binary alloys, statistical analyses broadly constrain order–disorder transition temperatures to about (0.3–0.45) T_m (where T_m is the melting temperature).[19,45,117–120] For CrCoNi ($T_m \approx 1700$ K), this corresponds to a transition temperature of 500–800 K. Similar temperature ranges likely apply to other 3*d* transition metal MPEAs with comparable T_m values, while refractory HEAs ($T_m > 2000$ K) would require higher optimal ordering temperatures. However, these correlations remain empirical approximations lacking mechanistic foundations. The persistent ambiguity and controversy surrounding SRO formation criteria in MPEAs primarily stem from inherent characterization challenges, as elaborated in Sec. V.

D. Effects of plastic deformation and irradiation on SRO

The formation and annihilation of SRO in MPEAs are fundamentally governed by the entropy–enthalpy competition within these systems, and it seems natural that suitable thermal processing could provide a wide range of degrees of SRO to modulate. Conventional wisdom suggests that alternative physical modification techniques such as severe plastic deformation (SPD) and irradiation primarily introduce structural defects and suppress the development of SRO, but some recent experimental results on MPEAs have challenged such statements.

For example, Seol *et al.*[121] demonstrated a strain-rate-controlled mechanically derived ordering in $Fe_{40}Mn_{40}Cr_{10}Co_{10}$ through *in situ* tensile testing at 77 K, where dislocation slip activation under constrained thermal conditions paradoxically enhanced SRO formation. Irradiation has long been recognized to have dual modulation effects in binary alloy systems: chemical disordering induced by cascade displacement and chemical ordering facilitated through thermally activated atom diffusion. While irradiation predominantly introduces defects and disrupts pre-existing ordered structures, it has been reported that in some binary systems, such as Ni–Al and Fe–Cr alloys, high-temperature irradiation could enable ordering or phase precipitation.[67,122,123] Research on the irradiation resistance of CrMnFeCoNi and such Cantor-derived alloys by He, Zhang, Zhou, Su, and co-workers[15,124–127] revealed that ion irradiation could assist or even dominate the formation of SRO in CrCoNi and CrMnFeCoNi, whereas CrFeCoNi was reported to remain stable in the disordered state after irradiation. Such ordering arose from the alteration of the kinetic behavior of defects and SRO under irradiation conditions. This radiation-assisted ordering effectively suppressed the formation and evolution of defects from irradiation. These reports have revealed that both tensile deformation and irradiation can provide activation energy for SRO formation or accelerate atomic diffusion processes.[128] This enables the realization of ordering that would otherwise remain frozen at lower temperatures, ultimately driving the system toward stable ordered states at low temperatures. These findings offer new perspectives on the interplay between thermodynamic formation conditions and kinetic constraints during SRO evolution in MPEAs.

V. CHARACTERIZATION OF SRO IN MPEAs

In binary alloys, as mentioned before, several well-established methods from multiple perspectives exist to characterize SRO. However, for MPEAs, the quantitative characterization of SRO remains highly controversial. Even some long-standing characterization approaches have recently been found insufficient to qualitatively confirm the existence of SRO.

A. X-ray-based atomic structural characterization

X-ray-based techniques represent the most common quantitative or qualitative characterization methods for SRO in binary systems. Although attempts to clarify the degree of pair-correlated SRO through X-ray diffuse scattering experiments have been proven exceptionally challenging in MPEAs, particularly in quaternary or quinary systems, Schönfeld *et al.*[129] successfully identified a tendency of L12-type SRO with Cr atoms at core positions in CrFeCoNi alloy by performing elastic diffuse scattering experiments with incident X-ray energy tuned near the absorption edges of the constituent elements to enhance the pairwise scattering contrast. By contrast, Li *et al.*[18] reported no diffuse scattering signals related to SRO in single-crystal XRD measurements of CrCoNi after annealing to optimize SRO.

Given the challenges in synthesizing single-crystal MPEA samples for certain compositions, X-ray-based characterization techniques using powder or polycrystalline samples have been extensively employed. In most 3*d* transition MPEAs, SRO is often not closely related to Fe, which renders the ^{57}Fe Mössbauer spectroscopic characterization conducted in binary alloys such as Fe–Cr and Fe–Al unsuitable for characterizing locally ordered structures in MPEAs, while EXAFS is still applicable. Despite its substantial uncertainties during data fitting and recognized fitting model-dependent nature, EXAFS is widely regarded as a powerful element-specific technique for characterizing real-space radial atomic pair distributions.[130,131] Although Zhang *et al.*[15,132] obtained ambiguous SRO signals for CrMnFeCoNi by EXAFS, they successfully captured evidence of SRO in CrCoNi.

Although conventional wisdom holds that detecting nanoprecipitates via powder diffraction is relatively straightforward, while capturing SRO signals remains challenging, recent advances combining total scattering PDF experiments with RMC fitting have successfully identified SRO in binary alloys.[39,40] Similar approaches have been extended to CrMnFeCoNi for analyzing lattice distortions and potential SRO.[133] Notably, He *et al.*[134] revealed SRO coupled with lattice distortion in CrFeCoNi through PDF experiments. Furthermore, although small-angle X-ray scattering (SAXS) may not

be suitable for 3*d* transition MPEA systems with minimal electron density contrast, it shows potential for characterizing local ordering in refractory MPEA systems with significant electron density differences.[135] Collectively, non-imaging X-ray techniques provide substantial indirect evidence for SRO in MPEAs. However, compositional complexity and methodological limitations often restrict conclusions to qualitative levels rather than quantitative or definitive proof.

B. Local magnetic structure characterization by X-ray spectroscopy and neutron scattering

Given that fcc-structured Cantor-derived 3*d* transition metal MPEAs contain multiple magnetic 3*d* transition elements, where Fe, Co, and Ni tend to form local ferromagnetic moments and Cr and Mn favor antiferromagnetic arrangements, it becomes evident that magnetism could influence local ordering structures.[104] This viewpoint has gained support from computational analyses by Woodgate *et al.*,[104] Niu *et al.*,[106] and Ghosh *et al.*[136]

X-ray absorption spectroscopy (XAS)-derived X-ray magnetic circular dichroism (XMCD) experiments employing soft X-ray photons with different helicities have been implemented to characterize element-specific local magnetic configurations in some Cantor-derived 3*d* transition MPEAs, which may potentially correlate with local atomic structures.[137,138] Neutron scattering is another powerful tool for observing the local magnetic order related to atomic SRO. These techniques have been employed by Billington *et al.*[137] and Zhu *et al.*,[139] respectively, to confirm magnetic ordering in various Cantor-derived alloys at low temperatures. Notably, the results of inelastic neutron scattering (INS) from Zhu *et al.*[139] have revealed persistent local spin fluctuations in CrMnFeCoNi even at ~200 K, suggesting potential magnetic-related SRO existence at higher temperatures. Nevertheless, significant contradictions remain in the reported low-temperature magnetic behaviors of Cantor alloys, with conflicting observations of antiferromagnetic, ferromagnetic, and spin-glass transitions at different critical temperatures.[137,139–142] In 3*d* transition MPEAs, the relationship between local magnetic structures and atomic SRO remains a critical consideration, requiring careful evaluation and further experimental confirmation.

C. Transmission electron microscopy

Conventional dark-field imaging in transmission electron microscopy (TEM) has long been employed to observe long-range ordering, particularly in nanoscale precipitation phases. In MPEA studies, the use of aberration-corrected high-angle annular dark-field scanning TEM (HAADF-STEM), together with atomic-resolution energy-dispersive X-ray spectroscopy (EDS) mapping techniques, has enabled characterization of nanoscale ordered structures with significant diffraction contrast, such as ordered oxygen complexes in oxygen-doped TiZrHfNb alloys reported by Lei *et al.*[143] and nanoscale compositional undulations in CrFeCoNiPd observed by Ding *et al.*[4] Nevertheless, imaging of SRO domains remains challenging because of their small sublattice size and diffuse characteristics. Particularly for 3*d* transition metal MPEAs, similarities in diffraction contrasts due to similar neighboring atomic number *Z* further obscure evidence of SRO. Recent advances in aberration correction and contrast optimization techniques, notably through the implementation of energy filters and nano-focused electron beams, have demonstrated promising potential for directly observing SRO using HAADF-STEM. Such techniques were initially developed for direct observation of SRO in Ti–6Al binary alloy and later applied to SRO in MPEAs.[144] In selected area electron diffraction (SAED) patterns, weak diffuse scattering intensities caused by compositional fluctuations have been observed in MEAs such as CrCoNi and VCoNi with fcc structures, as well as in typical fcc-structured HEAs such as CrMnFeCoNi and its derived alloys, and bcc-structured MPEA such as TiZrNbVAl.[2,3,121,125,145–147] In these cases, real-space dark-field imaging results remain ambiguous, with primary evidence for SRO derived from diffuse scattering intensities in reciprocal-space diffraction patterns along specific zone axes. These diffuse intensities generally manifest as two types: diffuse streaks connecting Bragg spots, and diffuse intensities at superstructure reciprocal lattice positions. Although limited by the HRTEM field of view and potentially lacking statistical significance, this approach can provide qualitative or semiquantitative confirmation of SRO in MPEAs.

However, recent studies have questioned whether these diffuse intensities truly originate from SRO in fcc-structured MPEAs.[17,20] Investigations have revealed that even in TEM SAED patterns of pure Cu or Ni, similar diffuse scattering features can be observed along a specific zone axis.[18] These extra intensities can also stem from various factors unrelated to SRO. Such experimentally observed diffuse scattering characteristics may also be matched with artifacts from aperiodic surface structures in TEM specimens, higher-order Laue zone (HOLZ) reflections, or misinterpretations of nanoscale symmetry-breaking defects. Notably, such artifacts are specifically associated with fcc-structural characteristics, thereby preserving the analytical validity of bcc-structured MPEAs. To effectively capture signals of SRO, it is essential to ensure the preparation of high-quality TEM samples while minimizing potential artifacts during characterization processes.

Considering that conventional TEM characterization can only capture averaged information from atomic column arrays along a specific zone axis, the uncertainty of atomic spatial coordinates in 3D real space also contributes to the aforementioned artifacts. Therefore, attempting to perform 3D atomic-resolution imaging based on TEM techniques could potentially serve as an effective approach for SRO. Recently, with the use of atomic electron tomography (AET), which allows 3D tomographic reconstruction from scanning transmission electron microscopy (STEM) images at different tilt angles, SRO and local lattice distortion of NiPdPt-based MPEAs have been quantitatively characterized.[148] Nevertheless, a persistent limitation of AET still lies in its insusceptibility to subtle variations in electron diffraction contrast coming from similar atomic number *Z*.

D. Atom probe tomography

An alternative approach involving 3D reconstruction to characterize SRO is atom probe tomography (APT).[28] In APT measurements, surface atoms from a needle-shaped specimen under a positive electrical potential undergo ionization and evaporation toward a detector. Each ion type can be determined by time of flight, and the detector can provide an accurate spatial position. APT can offer high chemical and spatial resolution, enabling direct imaging of atomic clusters comprising only a few atoms. Notably,

it stands as the sole experimental technique currently capable of quantifying GM-SRO parameters in multiple-component systems. Nevertheless, two primary technical constraints may impede its precision in SRO characterization: first, the finite detection efficiency restricts the complete detection of evaporated ions; second, the limited spatial resolution of detectors and uncertainties in trajectory result in blurring of the local crystalline atomic structure. To address these intrinsic limitations, several methodological refinements to APT experiments and data reconstruction algorithms are being actively implemented in MPEA investigations to distinguish SRO from random configurations.[29,109,112,143,149] It seems that APT demonstrates significant potential as a composition-sensitive characterization technique to confirm the validity of SRO signals derived from scattering experiments.

E. Yield strength

Beyond direct structural characterization through X-ray, electron, and neutron scattering, investigations of SRO in MPEAs have been largely motivated by its substantial influence on mechanical properties. This naturally prompts consideration of mechanical testing as a qualitative/semiquantitative SRO assessment method. However, a critical challenge persists: To what extent can SRO genuinely modify the mechanical performance of MPEAs? Current findings remain contentious. Zhang *et al.* reported notable SRO effects in CrCoNi,[2,110] and Yin *et al.*[16] observed minimal mechanical property variations attributable to SRO. In particular, in annealing experiments designed to manipulate SRO levels and mechanical responses in CrCoNi, the first pop-in load in nanoindentation tests exhibited high sensitivity to heat treatment parameters, potentially providing an effective indicator for correlating annealing temperature, SRO degree, and mechanical properties. Nevertheless, reported optimal annealing temperatures for maximizing the first pop-in load vary dramatically from 1073 to 673 K.[19] This discrepancy may stem not only from an incomplete understanding of SRO formation conditions in early studies, but also from synergistic contributions of multiple strengthening mechanisms in CrCoNi-type MPEAs. Therefore, direct mechanical property-based characterization of SRO shows promise, but challenges remain, and complementary verification through different techniques is required.

F. Stacking fault energy

A potential alternative approach for qualitative SRO assessment involves establishing correlations between SRO and stacking fault energy (SFE) with associated fcc–hcp (hexagonal close-packed) phase transition mechanisms. Computational studies suggest that SRO can significantly modify SFE in fcc systems (although SFE in bcc crystals typically remains too high for stacking fault formation), even reversing its sign.[97] SFE quantification traditionally relies on measuring stacking fault widths by TEM or on observations of the widening and shifting of diffraction peaks by XRD. In the case of TEM, this method becomes unreliable for negative SFE values and suffers from statistical limitations due to the varying concentrations of local SRO. In the case of XRD, the effects of SFE on profile peaks can be rather difficult to distinguish from microstrains and crystal grain size.[150–152] Moreover, in an fcc crystal, stacking faults can be considered as the thinnest hcp lamellae, composed of two atomic hcp layers. Decreasing SFE drives deformation mode transitions from dislocation gliding to mechanical twinning and ultimately to fcc–hcp martensitic transitions.[97] Recent investigations have identified SFE as a critical factor governing fcc–hcp pressure-induced phase transitions in MPEAs.[153] However, establishing reliable experimental correlations between SFE and SRO remains an ongoing challenge requiring further exploration.

G. Resistometry

In binary alloy systems, resistivity and thermodynamic tests have long been recognized as valid methods for quantifying both LRO and SRO. While LRO formation typically reduces resistivity, SRO generally exhibits the opposite trend. By tailoring compositions to introduce ordered nanoprecipitates and SRO, Zhu *et al.*[93] achieved temperature-independent resistivity over a broad thermal range in a 3*d* transition metal-based MPEA. With regard to the specific correlation between SRO and resistivity, Schönfeld *et al.*[129] monitored the evolution of SRO and thermal equilibrium in CrFeCoNi alloy through resistivity changes of less than 2%. Li *et al.*[18] found that single-crystal specimens quenched after extended annealing (>100 h at 673 K) exhibited a ~5% resistivity enhancement, potentially indicating maximized SRO formation, as shown in Fig. 2.

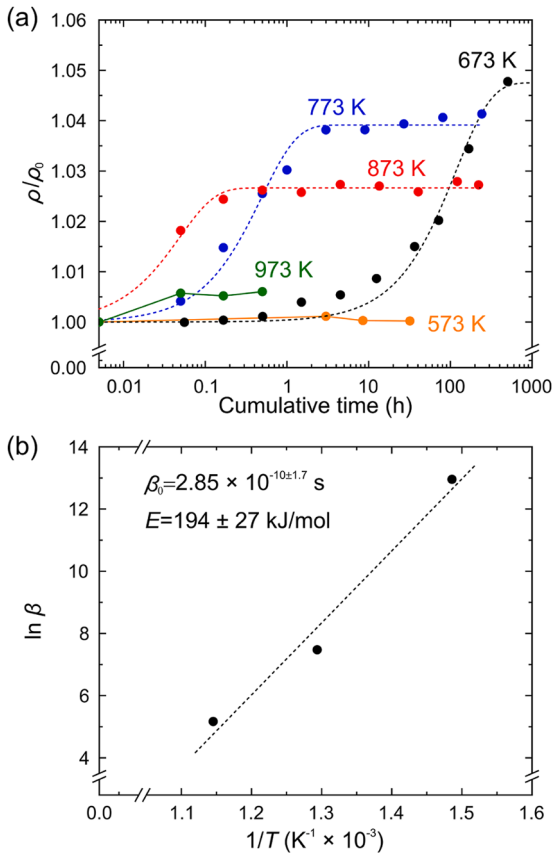

FIG. 2. Variations in electrical resistivity of equiatomic Cr–Co–Ni polycrystals quenched from 1473 K during isothermal annealing at various temperatures ranging from 573 to 973 K.[18]

Notably, the tendency of an increasing time-dependent resistivity can be described well by an Avrami-type equation with exponent $n = 1$:

$$\frac{\rho(t)}{\rho_0} = 1 + \delta\left[1 - \exp\left(-\frac{t^n}{\beta}\right)\right],$$

where t is the annealing time, and δ and β are constants depending on the annealing temperature. The value $n = 1$ of the Avrami index suggests that the growth of CrCoNi is non-isotropic and needle-like.[154,155] These resistivity-based findings are intriguing, but critical considerations emerge. As highlighted by Tanimoto *et al.*[108] and Teramoto *et al.*,[107] a number of parameters, including quenching rate and temperature, significantly influence MPEA resistivity. Moreover, resistivity proves sensitive to extraneous factors such as impurity concentration, defect density, and grain boundary scattering, imposing stringent requirements on sample quality and experimental precision to enable a reliable SRO–resistivity correlation to be established.

H. Calorimetry

Thermodynamic characterization via DSC appears theoretically promising for SRO investigation, given the intrinsic entropy–enthalpy interplay. However, unlike rapid ordering or disordering processes in binary alloys or metallic glasses, MPEAs require hundreds of hours for potentially detectable SRO evolution, leading to pronounced thermal hysteresis and attenuated DSC signals. Although previous studies have employed DSC as supplementary evidence for SRO, the obtained signals remain ambiguous. Systematic work by Bacurau *et al.*[44] has revealed progressive disappearance of exothermic SRO formation signals and the emergence of high-temperature endothermic SRO dissolution peaks in CrCoNi during prolonged annealing, as shown in Fig. 3. Although these thermal signatures are quantifiable, their intensity remains orders of magnitude weaker than those observed in binary systems such as $CrNi_2$. Notably, the reported SRO initiation temperature of 748 K in this study differs from the 673 K optimal annealing temperature identified through resistivity measurements, highlighting persistent discrepancies in current SRO characterization methodologies.

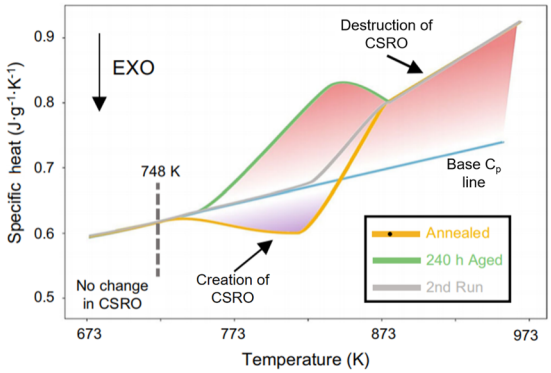

FIG. 3. Schematic of heat evolved during DSC testing of CrCoNi. Below around 748 K, the kinetics are too slow to change the CSRO on the experimental timescale. Above 748 K, CSRO can be either created (purple shading) or destroyed (red shading), as indicated by exothermic and endothermic reactions, respectively.[44]

VI. PERSPECTIVES AND SUMMARY

The investigation of SRO in MPEAs originated from demands for performance optimization. However, akin to the critical role of SRO as a fundamental crystallographic issue in binary alloys, advancing the understanding of SRO in MPEAs will deepen insights into entropy–enthalpy competition and its influence on microstructural evolution and phase stability. Regardless of its mechanical implications, SRO remains one of the most significant research topics in the MPEA field. In this review, we have identified the following unresolved challenges as requiring urgent attention:

1. Although systematic and precise characterization of SRO in MPEAs remains significantly challenging, the integration of meticulous scattering experiments with imaging techniques, combined with resistometry and calorimetry, has facilitated a comprehensive understanding of the existence of SRO in these complex systems.
2. However, the evolutionary mechanisms of SRO in MPEAs remain incompletely elucidated. In particular, the absence of an SRO–LRO transition and the critical controversies that remain regarding SRO formation conditions still require deeper exploration and clarification.
3. Given the entropy–enthalpy competition induced by the high configurational entropy in MPEA systems, SRO could be ubiquitous across various compositions. Nevertheless, the adjustable range of SRO in these alloys and the key factors influencing their tunability demand clarification. Most crucially, to what extent can optimized SRO enhance mechanical properties and other functional characteristics? Can the strength contribution from SRO compete with traditional strengthening mechanisms such as Hall–Petch strengthening? Addressing these fundamental questions may require systematic mechanical characterization predicated on accurate determination of SRO formation processes for verification.

ACKNOWLEDGMENTS

This work was supported by the Shanghai Key Laboratory of Material Frontiers Research in Extreme Environments, China (Grant No. 22dz2260800) and the Shanghai Science and Technology Committee, China (Grant No. 22JC1410300).

AUTHOR DECLARATIONS

Conflict of Interest

The authors have no conflicts to disclose.

Author Contributions

Yuxin Liu: Investigation (equal); Validation (equal); Writing – original draft (lead); Writing – review & editing (equal). **Hongbo Lou**:

Validation (equal); Writing – review & editing (equal). **Fei Zhang**: Validation (equal); Writing – review & editing (equal). **Zhidan Zeng**: Project administration (equal); Validation (equal); Writing – review & editing (equal). **Qiaoshi Zeng**: Conceptualization (lead); Funding acquisition (lead); Project administration (lead); Resources (lead); Supervision (lead); Validation (equal); Writing – review & editing (equal).

DATA AVAILABILITY

Data sharing is not applicable to this article as no new data were created or analyzed in this study.

REFERENCES

[1] N. Rasooli, W. Chen, and M. Daly, "Deformation mechanisms in high entropy alloys: A minireview of short-range order effects," Nanoscale **16**, 1650–1663 (2024).

[2] R. Zhang, S. Zhao, J. Ding, Y. Chong, T. Jia *et al.*, "Short-range order and its impact on the CrCoNi medium-entropy alloy," Nature **581**, 283–287 (2020).

[3] L. Wang, J. Ding, S. Chen, K. Jin, Q. Zhang *et al.*, "Tailoring planar slip to achieve pure metal-like ductility in body-centred-cubic multi-principal element alloys," Nat. Mater. **22**, 950–957 (2023).

[4] Q. Ding, Y. Zhang, X. Chen, X. Fu, D. Chen *et al.*, "Tuning element distribution, structure and properties by composition in high-entropy alloys," Nature **574**, 223–227 (2019).

[5] Q. F. He, J. G. Wang, H. A. Chen, Z. Y. Ding, Z. Q. Zhou *et al.*, "A highly distorted ultraelastic chemically complex Elinvar alloy," Nature **602**, 251–257 (2022).

[6] A. Manzoor, S. Pandey, D. Chakraborty, S. R. Phillpot, and D. S. Aidhy, "Entropy contributions to phase stability in binary random solid solutions," npj Comput. Mater. **4**, 47 (2018).

[7] F. Otto, Y. Yang, H. Bei, and E. P. George, "Relative effects of enthalpy and entropy on the phase stability of equiatomic high-entropy alloys," Acta Mater. **61**, 2628–2638 (2013).

[8] B. Zhang, J. Ding, and E. Ma, "Chemical short-range order in body-centered-cubic TiZrHfNb high-entropy alloys," Appl. Phys. Lett. **119**, 201908 (2021).

[9] Y. Wu, F. Zhang, X. Yuan, H. Huang, X. Wen *et al.*, "Short-range ordering and its effects on mechanical properties of high-entropy alloys," J. Mater. Sci. Technol. **62**, 214–220 (2021).

[10] L. Liu, Y. Zhang, J. Han, X. Wang, W. Jiang *et al.*, "Nanoprecipitate-strengthened high-entropy alloys," Adv. Sci. **8**, 2100870 (2021).

[11] K. Xun, B. Zhang, Q. Wang, Z. Zhang, J. Ding *et al.*, "Local chemical inhomogeneities in TiZrNb-based refractory high-entropy alloys," J. Mater. Sci. Technol. **135**, 221–230 (2023).

[12] H. Li, H. Zong, S. Li, S. Jin, Y. Chen *et al.*, "Uniting tensile ductility with ultrahigh strength via composition undulation," Nature **604**, 273–279 (2022).

[13] S. Chen, Z. H. Aitken, S. Pattamatta, Z. Wu, Z. G. Yu *et al.*, "Simultaneously enhancing the ultimate strength and ductility of high-entropy alloys via short-range ordering," Nat. Commun. **12**, 4953 (2021).

[14] Q.-J. Li, H. Sheng, and E. Ma, "Strengthening in multi-principal element alloys with local-chemical-order roughened dislocation pathways," Nat. Commun. **10**, 3563 (2019).

[15] F. Zhang, S. Zhao, K. Jin, H. Xue, G. Velisa *et al.*, "Local structure and short-range order in a NiCoCr solid solution alloy," Phys. Rev. Lett. **118**, 205501 (2017).

[16] B. Yin, S. Yoshida, N. Tsuji, and W. A. Curtin, "Yield strength and misfit volumes of NiCoCr and implications for short-range-order," Nat. Commun. **11**, 2507 (2020).

[17] F. G. Coury, C. Miller, R. Field, and M. Kaufman, "On the origin of diffuse intensities in fcc electron diffraction patterns," Nature **622**, 742–747 (2023).

[18] L. Li, Z. Chen, S. Kuroiwa, M. Ito, K. Yuge *et al.*, "Evolution of short-range order and its effects on the plastic deformation behavior of single crystals of the equiatomic Cr-Co-Ni medium-entropy alloy," Acta Mater. **243**, 118537 (2023).

[19] L. Li, J.-P. Du, S. Ogata, and H. Inui, "Variation of first pop-in loads in nanoindentation to detect chemical short-range ordering in the equiatomic Cr-Co-Ni medium-entropy alloy," Acta Mater. **269**, 119775 (2024).

[20] F. Walsh, M. Zhang, R. O. Ritchie, M. Asta, and A. M. Minor, "Multiple origins of extra electron diffractions in fcc metals," Sci. Adv. **10**, eadn9673 (2024).

[21] F. Walsh, A. Abu-Odeh, and M. Asta, "Reconsidering short-range order in complex concentrated alloys," MRS Bull. **48**, 753–761 (2023).

[22] J. M. Cowley, "X-ray measurement of order in single crystals of Cu_3Au," J. Appl. Phys. **21**, 24 (1950).

[23] D. T. Keating and B. E. Warren, "Long-range order in beta-brass and Cu_3Au," J. Appl. Phys. **22**, 286 (1951).

[24] J. M. Cowley, "Short- and long-range order parameters in disordered solid solutions," Phys. Rev. **120**, 1648 (1960).

[25] C. Wolverton, V. Ozolins, and A. Zunger, "Short-range-order types in binary alloys: A reflection of coherent phase stability," J. Phys. Condens. Matter **12**, 2749 (2000).

[26] J. Kanamori and Y. Kakehashi, "Conditions for the existence of ordered structure in binary alloy systems," J. Phys., Colloq. **38**, C7-274–C7-279 (1977).

[27] A. V. Ceguerra, M. P. Moody, R. C. Powles, T. C. Petersen, R. K. W. Marceau *et al.*, "Short-range order in multicomponent materials," Acta Crystallogr., Sect. A:Found. Crystallogr. **68**, 547–560 (2012).

[28] R. K. W. Marceau, A. V. Ceguerra, A. J. Breen, D. Raabe, and S. P. Ringer, "Quantitative chemical-structure evaluation using atom probe tomography: Short-range order analysis of Fe–Al," Ultramicroscopy **157**, 12–20 (2015).

[29] M. He, W. J. Davids, A. J. Breen, and S. P. Ringer, "Quantifying short-range order using atom probe tomography," Nat. Mater. **23**, 1200–1207 (2024).

[30] F. Solal, R. Caudron, F. Ducastelle, A. Finel, and A. Loiseau, "Long-range order and short-range order in Pd_3 V: Breakdown of the mean-field theory," Phys. Rev. Lett. **58**, 2245 (1987).

[31] Z. W. Lu and A. Zunger, "Unequal wave vectors in short- versus long-range ordering in intermetallic compounds," Phys. Rev. B **50**, 6626 (1994).

[32] F. Solal, R. Caudron, and A. Finel, "In situ diffuse neutron scattering on disordered Pd_3V and Ni_3V," Physica B **156–157**, 75–77 (1989).

[33] C. Wolverton and A. Zunger, "First-principles theory of short-range order, electronic excitations, and spin polarization in Ni-V and Pd-V alloys," Phys. Rev. B **52**, 8813 (1995).

[34] C. Wolverton, V. Ozoliņš, and A. Zunger, "First-principles theory of short-range order in size-mismatched metal alloys: Cu-Au, Cu-Ag, and Ni-Au," Phys. Rev. B **57**, 4332 (1998).

[35] C. Wolverton and A. Zunger, "Ising-like description of structurally relaxed ordered and disordered alloys," Phys. Rev. Lett. **75**, 3162 (1995).

[36] B. Schönfeld, M. Portmann, S. Yu, and G. Kostorz, "The type of order in Cu–10 at.% Au—evidence from the diffuse scattering of X-rays," Acta Mater. **47**, 1413–1416 (1999).

[37] V. Ozoliņš, C. Wolverton, and A. Zunger, "Cu-Au, Ag-Au, Cu-Ag, and Ni-Au intermetallics: First-principles study of temperature-composition phase diagrams and structures," Phys. Rev. B **57**, 6427 (1998).

[38] B. Schönfeld, "Local atomic arrangements in binary alloys," Prog. Mater. Sci. **44**, 435–543 (1999).

[39] L. R. Owen, H. Y. Playford, H. J. Stone, and M. G. Tucker, "Analysis of short-range order in Cu_3Au using X-ray pair distribution functions," Acta Mater. **125**, 15–26 (2017).

[40] L. R. Owen, H. Y. Playford, H. J. Stone, and M. G. Tucker, "A new approach to the analysis of short-range order in alloys using total scattering," Acta Mater. **115**, 155–166 (2016).

[41] R. Feder, M. Mooney, and A. S. Nowick, "Ordering kinetics in long-range ordered Cu_3Au," Acta Metall. **6**, 266–277 (1958).

[42] T. Hashimoto, K. Nishimura, and Y. Takeuchi, "Dynamics on transitional ordering process in Cu_3Au alloy from disordered state to ordered state," J. Phys. Soc. Jpn. **45**, 1127–1135 (1978).

[43] P. Bardhan and J. B. Cohen, "A structural study of the alloy Cu_3Au above its critical temperature," Acta Crystallogr., Sect. A:Found. Crystallogr. **32**, 597–614 (1976).

[44]V. P. Bacurau, P. A. F. P. Moreira, G. Bertoli, A. F. Andreoli, E. Mazzer *et al.*, "Comprehensive analysis of ordering in CoCrNi and $CrNi_2$ alloys," Nat. Commun. **15**, 7815 (2024).
[45]A. Marucco, "Atomic ordering and α′-Cr phase precipitation in long-term aged Ni_3Cr and Ni_2Cr alloys," J. Mater. Sci. **30**, 4188–4194 (1995).
[46]R. K. W. Marceau, A. V. Ceguerra, A. J. Breen, M. Palm, F. Stein *et al.*, "Atom probe tomography investigation of heterogeneous short-range ordering in the 'komplex' phase state (K-state) of Fe–18Al (at.%)," Intermetallics **64**, 23–31 (2015).
[47]N. V. Ershov, Y. P. Chernenkov, V. A. Lukshina, and O. P. Smirnov, "Short-range order in α-FeAl soft magnetic alloy," Phys. Solid State **60**, 1661–1673 (2018).
[48]V. Pierron-Bohnes, S. Lefebvre, M. Bessiere, and A. Finel, "Short range order in a single crystal of Fe-19.5 at.% Al in the ferromagnetic range measured through X-ray diffuse scattering," Acta Metall. Mater. **38**, 2701–2710 (1990).
[49]I. Mirebeau, M. Hennion, and G. Parette, "First measurement of short-range-order inversion as a function of concentration in a transition alloy," Phys. Rev. Lett. **53**, 687 (1984).
[50]S. M. Dubiel and J. Zukrowski, "Phase-decomposition-related short-range ordering in an Fe–Cr alloy," Acta Mater. **61**, 6207–6212 (2013).
[51]M. Liu, A. Aiello, Y. Xie, and K. Sieradzki, "The effect of short-range order on passivation of Fe-Cr alloys," J. Electrochem. Soc. **165**, C830 (2018).
[52]I. Mirebeau and G. Parette, "Neutron study of the short range order inversion in $Fe_{1-x}Cr_x$," Phys. Rev. B **82**, 104203 (2010).
[53]S. M. Dubiel and J. Cieslak, "Short-range order in iron-rich Fe-Cr alloys as revealed by Mössbauer spectroscopy," Phys. Rev. B **83**, 180202 (2011).
[54]E. P. Yelsukov, E. V. Voronina, and V. A. Barinov, "Mössbauer study of magnetic properties formation in disordered Fe-Al alloys," J. Magn. Magn Mater. **115**, 271–280 (1992).
[55]S. C. Moss, "X-ray measurement of short range order in Cu_3Au," J. Appl. Phys. **35**, 3547–3553 (1964).
[56]H. Reichert, S. C. Moss, and K. S. Liang, "Anomalous temperature dependence of the X-ray diffuse scattering intensity of Cu_3Au," Phys. Rev. Lett. **77**, 4382 (1996).
[57]M. Bessière, S. Lefebvre, and Y. Calvayrac, "X-ray diffraction study of short-range order in a disordered Au_3Cu alloy," Struct. Sci. **39**, 145–153 (1983).
[58]S. Hashimoto and S. Ogawa, "Electron diffraction study on diffuse scattering from disordered Cu_3Au alloy," J. Phys. Soc. Jpn. **29**, 710–721 (1970).
[59]S. C. Moss and R. H. Walker, "Screening singularities and Fermi surface effects in the diffuse scattering from alloys," J. Appl. Crystallogr. **8**, 96–107 (1975).
[60]I. Tsatskis, "Non-mean-field theories of short range order and diffuse scattering anomalies in disordered alloys," in *Local Structure from Diffraction* (Springer, 1998), pp. 207–231.
[61]T. R. Welberry, *Diffuse X-Ray Scattering and Models of Disorder* (Oxford University Press, 2022).
[62]M. Bessiere, E. Dartyge, and S. Lefebvre, "Study of short range order in Au_3 Cu by EXAFS," J. Phys., Colloq. **47**, C8-1033–C8-1036 (1986).
[63]T. K. Sham, A. Hiraya, and M. Watanabe, "Electronic structure of Cu-Au alloys from the Cu perspective: A Cu $L_{3,2}$-edge study," Phys. Rev. B **55**, 7585 (1997).
[64]Y. A. Babanov, A. V. Ryazhkin, T. Miyanaga, T. Okazaki, A. F. Sidorenko *et al.*, "Short range order in disordered Ni–Mn alloys by EXAFS," Nucl. Instrum. Methods Phys. Res., Sect. A **448**, 364–367 (2000).
[65]A. I. Ismail and R. Haliq, "Influence of Cr-content on the local atomic structure of Fe–Cr alloy, a study using EXAFS," Radiat. Phys. Chem. **208**, 110869 (2023).
[66]W. Schweika and H.-G. Haubold, "Neutron-scattering and Monte Carlo study of short-range order and atomic interaction in $Ni_{0.89}Cr_{0.11}$," Phys. Rev. B **37**, 9240 (1988).
[67]N. Filippova, V. Shabashov, and A. Nikolaev, "Mossbauer study of irradiation-accelerated short-range ordering in binary Fe-Cr alloys," Phys. Met. Metallogr. **90**, 145–152 (2000).
[68]H. Thomas, "Über widerstandslegierungen," Z. Phys. **129**, 219–232 (1951).
[69]R. G. Davies, "An X-ray and dilatometric study of order and the 'K-state' in iron-aluminum alloys," J. Phys. Chem. Solid. **24**, 985–992 (1963).
[70]R. J. Taunt and B. Ralph, "Ordering and the K-effect in Ni_2Cr," Phys. Status Solidi A **29**, 431–442 (1975).
[71]E. A. Starke, Jr., V. Gerold, and A. G. Guy, "An investigation of the *k*-effect in nickel-aluminum alloys," Acta Metall. **13**, 957–964 (1965).
[72]B. H. Rabin, W. D. Swank, and R. N. Wright, "Thermophysical properties of alloy 617 from 25 °C to 1000 °C," Nucl. Eng. Des. **262**, 72–80 (2013).
[73]H. J. Logie, J. Jackson, J. C. Anderson, and F. R. N. Nabarro, "Effect of plastic deformation on resistivity of gold-palladium alloys," Acta Metall. **9**, 707–713 (1961).
[74]E. Nagy and I. Nagy, "Ordering in alloy Cu_3Au—I," J. Phys. Chem. Solid. **23**, 1605–1612 (1962).
[75]P. Wright and J. C. Goodchild, "Vacancy induced ordering in Cu_3Au," Proc. Phys. Soc. **79**, 196 (1962).
[76]M. C. Franzblau and R. B. Gordon, "The order-disorder transformation in Cu_3Au at high pressure," J. Appl. Phys. **38**, 103–110 (1967).
[77]B. Sprusil, V. Sima, B. Chalupa, and B. Smola, "Phase transformations in CuAu and Cu_3Au: A comparison between calorimetric and resistometric measurements/Phasenumwandlungen in CuAu und Cu_3Au: ein Vergleich zwischen kalorimetrischen und resistometrischen Messungen," Int. J. Mater. Res. **84**, 118–123 (1993).
[78]A. Benisek and E. Dachs, "The vibrational and configurational entropy of disordering in Cu_3Au," J. Alloys Compd. **632**, 585–590 (2015).
[79]A. Benisek, E. Dachs, and M. Grodzicki, "Vibrational entropy of disorder in Cu_3Au with different degrees of short-range order," Phys. Chem. Chem. Phys. **20**, 19441–19446 (2018).
[80]L. J. Nagel, L. Anthony, and B. Fultz, "Differences in vibrational entropy of disordered and ordered Cu_3Au," Philos. Mag. Lett. **72**, 421–427 (1995).
[81]A. Marucco and B. Nath, "Effects of ordering on the properties of Ni-Cr alloys," J. Mater. Sci. **23**, 2107–2114 (1988).
[82]M. Hirabayashi, M. Koiwa, K. Tanaka, T. Tadaki, T. Saburi *et al.*, "An experimental study on the ordered alloy Ni_2Cr," Trans. Jpn. Inst. Metals **10**, 365–371 (1969).
[83]N. R. Dudova and R. O. Kaibyshev,"Short-range ordering and mechanical properties of a Ni-20%Cr alloy," J. Phys.: Conf. Ser. **240**, 012081 (2010).
[84]P. Singh, A. V. Smirnov, and D. D. Johnson, "Atomic short-range order and incipient long-range order in high-entropy alloys," Phys. Rev. B **91**, 224204 (2015).
[85]J. Tian, Y. Wu, T. Cao, J. Pang, X. Zhang *et al.*, "Fast and diverse phase evolution in VCoNi medium entropy alloy," Mater. Sci. Eng. A **860**, 144277 (2022).
[86]T. H. Chou, W. P. Li, L. Y. Zhu, F. Zhu, X. C. Li *et al.*, "Critical impacts of thermodynamic instability and short-range order on deformation mechanisms of VCoNi medium-entropy alloy," Acta Mater. **277**, 120190 (2024).
[87]M. Vaidya, K. Guruvidyathri, and B. S. Murty, "Phase formation and thermal stability of CoCrFeNi and CoCrFeMnNi equiatomic high entropy alloys," J. Alloys Compd. **774**, 856–864 (2019).
[88]H. Hamdi, H. R. Abedi, and Y. Zhang, "A review study on thermal stability of high entropy alloys: Normal/abnormal resistance of grain growth," J. Alloys Compd. **960**, 170826 (2023).
[89]D. Ma, M. Yao, K. G. Pradeep, C. C. Tasan, H. Springer *et al.*, "Phase stability of non-equiatomic CoCrFeMnNi high entropy alloys," Acta Mater. **98**, 288–296 (2015).
[90]Y. Wu, Z. Li, H. Feng, and S. He, "Atomic interactions and order–disorder transition in FCC-type $FeCoNiAl_{1-x}Ti_x$ high-entropy alloys," Materials **15**, 3992 (2022).
[91]Y. Ma, J. Fan, L. Zhang, M. Zhang, P. Cui *et al.*, "Pressure-induced ordering phase transition in high-entropy alloy," Intermetallics **103**, 63–66 (2018).
[92]F. Zhang, H. Lou, B. Cheng, Z. Zeng, and Q. Zeng, "High-pressure induced phase transitions in high-entropy alloys: A review," Entropy **21**, 239 (2019).
[93]S. Zhu, D. Yan, Y. Zhang, L. Han, D. Raabe *et al.*, "Strong and ductile Resinvar alloys with temperature- and time-independent resistivity," Nat. Commun. **15**, 7199 (2024).
[94]M. E. Bloomfield, K. A. Christofidou, P. M. Mignanelli, A.-P. M. Reponen, H. J. Stone *et al.*, "Phase stability of the $Al_xCrFeCoNi$ alloy system," J. Alloys Compd. **926**, 166734 (2022).
[95]C. Li, M. Zhao, J. C. Li, and Q. Jiang, "*B*2 structure of high-entropy alloys with addition of Al," J. Appl. Phys. **104**, 113504 (2008).

[96]Y. Ma, B. Jiang, C. Li, Q. Wang, C. Dong *et al.*, "The BCC/B2 morphologies in Al_xNiCoFeCr high-entropy alloys," Metals **7**, 57 (2017).
[97]J. Ding, Q. Yu, M. Asta, and R. O. Ritchie, "Tunable stacking fault energies by tailoring local chemical order in CrCoNi medium-entropy alloys," Proc. Natl. Acad. Sci. U. S. A. **115**, 8919–8924 (2018).
[98]Y. Zhang, Y. N. Osetsky, and W. J. Weber, "Tunable chemical disorder in concentrated alloys: Defect physics and radiation performance," Chem. Rev. **122**, 789–829 (2021).
[99]X. D. Xu, P. Liu, S. Guo, A. Hirata, T. Fujita *et al.*, "Nanoscale phase separation in a fcc-based CoCrCuFeNi$Al_{0.5}$ high-entropy alloy," Acta Mater. **84**, 145–152 (2015).
[100]A. Fantin, G. O. Lepore, A. M. Manzoni, S. Kasatikov, T. Scherb *et al.*, "Short-range chemical order and local lattice distortion in a compositionally complex alloy," Acta Mater. **193**, 329–337 (2020).
[101]Y. Tong, S. Zhao, H. Bei, T. Egami, Y. Zhang *et al.*, "Severe local lattice distortion in Zr- and/or Hf-containing refractory multi-principal element alloys," Acta Mater. **183**, 172–181 (2020).
[102]F. Körmann, A. V. Ruban, and M. H. Sluiter, "Long-ranged interactions in bcc NbMoTaW high-entropy alloys," Mater. Res. Lett. **5**, 35–40 (2017).
[103]F. Walsh, M. Asta, and R. O. Ritchie, "Magnetically driven short-range order can explain anomalous measurements in CrCoNi," Proc. Natl. Acad. Sci. U. S. A. **118**, e2020540118 (2021).
[104]C. D. Woodgate, D. Hedlund, L. H. Lewis, and J. B. Staunton, "Interplay between magnetism and short-range order in medium- and high-entropy alloys: CrCoNi, CrFeCoNi, and CrMnFeCoNi," Phys. Rev. Mater. **7**, 053801 (2023).
[105]C. Niu, A. J. Zaddach, A. A. Oni, X. Sang, J. W. Hurt III *et al.*, "Spin-driven ordering of Cr in the equiatomic high entropy alloy NiFeCrCo," Appl. Phys. Lett. **106**, 161906 (2015).
[106]C. Niu, C. R. LaRosa, J. Miao, M. J. Mills, and M. Ghazisaeidi, "Magnetically-driven phase transformation strengthening in high entropy alloys," Nat. Commun. **9**, 1363 (2018).
[107]T. Teramoto, K. Kitasumi, R. Shimohara, Y. Ito, R. Shimizu *et al.*, "Formation condition and effect on the early stages of plastic deformation of chemical short-range order in Cr-Co-Ni medium-entropy alloy," J. Alloys Compd. **941**, 169016 (2023).
[108]H. Tanimoto, R. Hozumi, and M. Kawamura, "Electrical resistivity and short-range order in rapid-quenched CrMnFeCoNi high-entropy alloy," J. Alloys Compd. **896**, 163059 (2022).
[109]K. Inoue, S. Yoshida, and N. Tsuji, "Direct observation of local chemical ordering in a few nanometer range in CoCrNi medium-entropy alloy by atom probe tomography and its impact on mechanical properties," Phys. Rev. Mater. **5**, 085007 (2021).
[110]M. Zhang, Q. Yu, C. Frey, F. Walsh, M. I. Payne *et al.*, "Determination of peak ordering in the CrCoNi medium-entropy alloy via nanoindentation," Acta Mater. **241**, 118380 (2022).
[111]L. Zhou, Q. Wang, J. Wang, X. Chen, P. Jiang *et al.*, "Atomic-scale evidence of chemical short-range order in CrCoNi medium-entropy alloy," Acta Mater. **224**, 117490 (2022).
[112]Y. Han, H. Chen, Y. Sun, J. Liu, S. Wei *et al.*, "Ubiquitous short-range order in multi-principal element alloys," Nat. Commun. **15**, 6486 (2024).
[113]E. Antillon, C. Woodward, S. I. Rao, B. Akdim, and T. A. Parthasarathy, "Chemical short range order strengthening in a model FCC high entropy alloy," Acta Mater. **190**, 29–42 (2020).
[114]D. V. Louzguine-Luzgin and J. Jiang, "On long-term stability of metallic glasses," Metals **9**, 1076 (2019).
[115]Y. Zhao, B. Shang, B. Zhang, X. Tong, H. Ke *et al.*, "Ultrastable metallic glass by room temperature aging," Sci. Adv. **8**, eabn3623 (2022).
[116]J. F. Radavich and A. Fort, "Effects of long-time exposure in alloy 625 at," Superalloys **718**, 635–647 (1994).
[117]P. Meisterle and W. Pfeiler, "Resistometric study of SRO-kinetics in α-AgAl," Acta Metall. **31**, 1543–1547 (1983).
[118]A. Y. Volkov, A. E. Kostina, E. G. Volkova, O. S. Novikova, and B. D. Antonov, "Microstructure and physicomechanical properties of a Cu-8 at % Pd alloy," Phys. Met. Metallogr. **118**, 1236–1246 (2017).
[119]R. G. Davies and R. W. Cahn, "Short range order in aluminium bronze," Acta Metall. **10**, 170–171 (1962).
[120]D. M. C. Nicholson and R. H. Brown, "Electrical resistivity of $Ni_{0.8}Mo_{0.2}$: Explanation of anomalous behavior in short-range ordered alloys," Phys. Rev. Lett. **70**, 3311 (1993).
[121]J. B. Seol, W.-S. Ko, S. S. Sohn, M. Y. Na, H. J. Chang *et al.*, "Mechanically derived short-range order and its impact on the multi-principal-element alloys," Nat. Commun. **13**, 6766 (2022).
[122]J.-H. Ke, E. R. Reese, E. A. Marquis, G. R. Odette, and D. Morgan, "Flux effects in precipitation under irradiation – Simulation of Fe-Cr alloys," Acta Mater. **164**, 586–601 (2019).
[123]Y. Zhao, A. Bhattacharya, C. Pareige, C. Massey, P. Zhu *et al.*, "Effect of heavy ion irradiation dose rate and temperature on α′ precipitation in high purity Fe-18%Cr alloy," Acta Mater. **231**, 117888 (2022).
[124]M.-R. He, S. Wang, S. Shi, K. Jin, H. Bei *et al.*, "Mechanisms of radiation-induced segregation in CrFeCoNi-based single-phase concentrated solid solution alloys," Acta Mater. **126**, 182–193 (2017).
[125]Z. Su, T. Shi, H. Shen, L. Jiang, L. Wu *et al.*, "Radiation-assisted chemical short-range order formation in high-entropy alloys," Scr. Mater. **212**, 114547 (2022).
[126]Z. Zhang, Z. Su, B. Zhang, Q. Yu, J. Ding *et al.*, "Effect of local chemical order on the irradiation-induced defect evolution in CrCoNi medium-entropy alloy," Proc. Natl. Acad. Sci. U. S. A. **120**, e2218673120 (2023).
[127]Y. Zhou, T. Shi, J. Li, L. Wu, Q. Peng *et al.*, "Element-dependent evolution of chemical short-range ordering tendency of NiCoFeCrMn under irradiation," Int. J. Plast. **171**, 103768 (2023).
[128]P. Cao, "How does short-range order impact defect kinetics in irradiated multiprincipal element alloys?," Acc. Mater. Res. **2**, 71–74 (2021).
[129]B. Schönfeld, C. R. Sax, J. Zemp, M. Engelke, P. Boesecke *et al.*, "Local order in Cr-Fe-Co-Ni: Experiment and electronic structure calculations," Phys. Rev. B **99**, 014206 (2019).
[130]H. Joress, B. Ravel, E. Anber, J. Hollenbach, D. Sur *et al.*, "Why is EXAFS for complex concentrated alloys so hard? Challenges and opportunities for measuring ordering with X-ray absorption spectroscopy," Matter **6**, 3763–3781 (2023).
[131]S. Calvin, *XAFS for Everyone* (CRC Press, 2024).
[132]F. Zhang, Y. Tong, K. Jin, H. Bei, W. J. Weber *et al.*, "Chemical complexity induced local structural distortion in NiCoFeMnCr high-entropy alloy," Mater. Res. Lett. **6**, 450–455 (2018).
[133]L. R. Owen, E. J. Pickering, H. Y. Playford, H. J. Stone, M. G. Tucker *et al.*, "An assessment of the lattice strain in the CrMnFeCoNi high-entropy alloy," Acta Mater. **122**, 11–18 (2017).
[134]Q. F. He, P. H. Tang, H. A. Chen, S. Lan, J. G. Wang *et al.*, "Understanding chemical short-range ordering/demixing coupled with lattice distortion in solid solution high entropy alloys," Acta Mater. **216**, 117140 (2021).
[135]S. D. Wang, X. J. Liu, Z. F. Lei, D. Y. Lin, F. G. Bian *et al.*, "Chemical short-range ordering and its strengthening effect in refractory high-entropy alloys," Phys. Rev. B **103**, 104107 (2021).
[136]S. Ghosh, K. Ueltzen, J. George, J. Neugebauer, and F. Körmann, "Chemical ordering and magnetism in face-centered cubic CrCoNi alloy," npj Comput. Mater. **10**, 284 (2024).
[137]D. Billington, A. D. N. James, E. I. Harris-Lee, D. A. Lagos, D. O'Neill *et al.*, "Bulk and element-specific magnetism of medium-entropy and high-entropy Cantor-Wu alloys," Phys. Rev. B **102**, 174405 (2020).
[138]A. Smekhova, A. Kuzmin, K. Siemensmeyer, C. Luo, J. Taylor *et al.*, "Local structure and magnetic properties of a nanocrystalline Mn-rich Cantor alloy thin film down to the atomic scale," Nano Res. **16**, 5626–5639 (2023).
[139]L. Zhu, H. He, M. Naeem, X. Sun, J. Qi *et al.*, "Antiferromagnetism and phase stability of CrMnFeCoNi high-entropy alloy," Phys. Rev. Lett. **133**, 126701 (2024).
[140]T. A. Elmslie, J. Startt, S. Soto-Medina, Y. Yang, K. Feng *et al.*, "Magnetic properties of equiatomic CrMnFeCoNi," Phys. Rev. B **106**, 014418 (2022).
[141]Ö. Özgün, D. Koch, A. Çakır, T. Tavşanoğlu, W. Donner *et al.*, "Magnetic properties of fcc and σ phases in equiatomic and off-equiatomic high-entropy Cantor alloys," Phys. Rev. B **106**, 214422 (2022).
[142]K. Jin, B. C. Sales, G. M. Stocks, G. D. Samolyuk, M. Daene *et al.*, "Tailoring the physical properties of Ni-based single-phase equiatomic alloys by modifying the chemical complexity," Sci. Rep. **6**, 20159 (2016).
[143]Z. Lei, X. Liu, Y. Wu, H. Wang, S. Jiang *et al.*, "Enhanced strength and ductility in a high-entropy alloy via ordered oxygen complexes," Nature **563**, 546–550 (2018).

[144]R. Zhang, S. Zhao, C. Ophus, Y. Deng, S. J. Vachhani *et al.*, "Direct imaging of short-range order and its impact on deformation in Ti-6Al," Sci. Adv. **5**, eaax2799 (2019).
[145]X. Chen, Q. Wang, Z. Cheng, M. Zhu, H. Zhou *et al.*, "Direct observation of chemical short-range order in a medium-entropy alloy," Nature **592**, 712–716 (2021).
[146]H.-W. Hsiao, R. Feng, H. Ni, K. An, J. D. Poplawsky *et al.*, "Data-driven electron-diffraction approach reveals local short-range ordering in CrCoNi with ordering effects," Nat. Commun. **13**, 6651 (2022).
[147]X. Chen, F. Yuan, H. Zhou, and X. Wu, "Structure motif of chemical short-range order in a medium-entropy alloy," Mater. Res. Lett. **10**, 149–155 (2022).
[148]S. Moniri, Y. Yang, J. Ding, Y. Yuan, J. Zhou *et al.*, "Three-dimensional atomic structure and local chemical order of medium- and high-entropy nanoalloys," Nature **624**, 564–569 (2023).
[149]Y. Li, Y. Wei, Z. Wang, X. Liu, T. Colnaghi *et al.*, "Quantitative three-dimensional imaging of chemical short-range order via machine learning enhanced atom probe tomography," Nat. Commun. **14**, 7410 (2023).
[150]X. Sun, S. Lu, R. Xie, X. An, W. Li *et al.*, "Can experiment determine the stacking fault energy of metastable alloys?," Mater. Des. **199**, 109396 (2021).
[151]Z. Zhang, J. Kou, L. Chen, J. Guo, X. Duan *et al.*, "From stacking fault to phase transformation: A quantitative model of plastic deformation of CoCrFeMnNi under different strain rates," Intermetallics **146**, 107585 (2022).
[152]P. Wu, Y. Zhang, L. Han, K. Gan, D. Yan *et al.*, "Unexpected sluggish martensitic transformation in a strong and super-ductile high-entropy alloy of ultralow stacking fault energy," Acta Mater. **261**, 119389 (2023).
[153]F. Zhang, H. Lou, Y. Liu, Z. Zeng, X. Chen *et al.*, "Compositional effect on pressure-induced polymorphism in high-entropy alloys," Mater. Today Chem. **42**, 102435 (2024).
[154]T. Pradell, D. Crespo, N. Clavaguera, and M. T. Clavaguera-Mora, "Diffusion controlled grain growth in primary crystallization: Avrami exponents revisited," J. Phys. Condens. Matter **10**, 3833 (1998).
[155]G. A. Young and D. R. Eno, "Long range ordering in model Ni-Cr-X alloys," in *Proceedings of the International Symposium Fontevraud* (Societe Francaise d'Energie Nucleaire, 2014), pp. 14–18.